Simen Owen Academic Proceedings Series

3rd International Conference on Electronics, Engineering, Computer Science and Applied Development (EESD 2026)

Article

Torque Transmission Efficiency of Magnetic Coupling Drives in Sealed Containers

Chuyang Jiang[1,*]

[1] A-Level International Curriculum Center, Harbin Engineering University, Harbin, China
* Correspondence: Chuyang Jiang, A-Level International Curriculum Center, Harbin Engineering University, Harbin, China

Abstract: Magnetic coupling drives provide a highly reliable, non-contact means of torque transmission for sealed containers, where conventional mechanical shaft penetration frequently introduces severe operational risks such as fluid leakage, environmental contamination, accelerated seal wear, and internal pressure instability. These characteristics make magnetic couplings relevant to demanding industrial applications, including sealed mixers, high-pressure vessels, chemical processing equipment, and laboratory reactors. However, existing performance evaluations predominantly focus on maximizing transmissible torque or optimizing static magnetic structure design. Consequently, the combined influence of the operational air gap, isolation wall thickness, dynamic load torque, and thermal loss on overall transmission efficiency remains insufficiently quantified. To address this limitation, this paper proposes a novel gap--wall--load calibrated evaluation framework. This approach seamlessly integrates analytical torque modeling, rigorous finite element calibration, dynamic slip-risk assessment, thermal-loss correction mechanisms, and repeated experimental validation procedures. Two public datasets, encompassing permanent magnet synchronous motor torque data and magnetic coupling coefficient data, are utilized with controlled laboratory bench testing to evaluate the proposed model's performance. Results demonstrate that the proposed framework significantly improves the calculated average efficiency from 77.9% ± 3.1% to 86.8% ± 1.7% on Dataset A, and from 75.6% ± 3.4% to 83.1% ± 1.9% on Dataset B, compared with the traditional cylindrical coupling baseline. Furthermore, the prediction error is substantially reduced to 4.9% ± 0.7% and 5.3% ± 0.8% across the two respective datasets. Ultimately, these findings strongly indicate that sealed-wall attenuation and load-dependent stability must be considered jointly when designing leakage-free magnetic coupling transmission systems.

Keywords: magnetic coupling; torque transmission; sealed containers; finite element analysis; thermal loss; slip risk

Received: 17 April 2026
Revised: 29 May 2026
Accepted: 10 June 2026
Published: 14 June 2026

1. Introduction

Magnetic coupling transmission transfers torque through magnetic interaction rather than direct mechanical shaft connection. It is suitable for sealed containers, pressure vessels, chemical reactors, vacuum chambers, and laboratory stirring systems where shaft openings may cause leakage, contamination, seal wear, or pressure instability [1]. Compared with conventional mechanical seals, magnetic coupling drives reduce direct contact at the sealing boundary and help maintain the integrity of closed systems. Therefore, improving torque transmission efficiency under sealed-container conditions is important for mechanical reliability and operational safety.

In practical applications, torque transmission efficiency is influenced by coupled factors, including air gap, isolation wall thickness, wall material, rotational speed, load

torque, and temperature rise. A thicker wall may improve sealing strength but weaken magnetic flux linkage. A larger air gap may reduce interference during assembly but decrease transmissible torque [1]. Higher speed may increase output capacity but also introduce torque fluctuation and thermal loss. These trade-offs make it insufficient to evaluate magnetic coupling performance only by nominal torque or maximum output torque.

Existing studies have examined magnetic drive pumps, permanent magnet couplings, and sealed transmission systems. However, several limitations remain [1]. Many studies focus on torque capacity or structural design, while efficiency loss caused by sealed walls and coupling gaps is not fully quantified. Air gap, wall thickness, and load torque are often analyzed separately, although they interact in actual sealed equipment. Some experiments are conducted under limited speed or load conditions, making stability under variable operating states unclear. In addition, thermal loss, torque fluctuation, and slip risk are not always included in performance evaluation.

To address these limitations, this paper investigates torque transmission efficiency of magnetic coupling drives in sealed containers through a combined modeling, simulation, and experimental framework. First, a gap--wall--load coupled efficiency model is established to describe how air gap, isolation wall thickness, and load torque jointly affect torque output and efficiency, and this model is verified through parameter-sensitivity experiments. Second, practical reliability indicators, including torque fluctuation rate, slip-risk coefficient, and thermal-loss correction, are introduced to evaluate stability under variable loads and speeds [2]. Third, the analytical model is calibrated using finite element simulation, and prediction error is evaluated against experimental measurements. Finally, a sealed-container test platform is used to collect input torque, output torque, speed, temperature, and load data under repeated experiments, with results compared against baseline coupling structures.

The technical route contains four steps: constructing a sealed-container magnetic coupling test system, developing an analytical torque transmission model, calibrating magnetic parameters through finite element simulation, and conducting repeated experiments under different gaps, wall thicknesses, speeds, and loads [3].

The academic value of this study lies in connecting magnetic coupling theory with sealed-container transmission considerations [4]. Practically, the results may support leakage-free transmission design for chemical processing, biomedical equipment, sealed mixers, and laboratory reactors. The proposed framework also improves interpretability because efficiency changes are explained through physical variables such as gap, wall thickness, load torque, and thermal loss.

2. Related Works

2.1. Magnetic Coupling Transmission

Magnetic coupling transmission has been widely studied as a non-contact torque transfer mechanism. Its main advantage is that torque can be transmitted without direct mechanical contact between the driving and driven shafts. This reduces wear, eliminates the need for a dynamic shaft seal, and enhances suitability for sealed or isolated environments. In magnetic drive pumps, sealed mixers, and small-scale stirring systems, magnetic coupling helps minimize leakage risk and maintenance demand [5].

However, existing studies often focus on maximum transmissible torque, magnetic pole arrangement, or structural optimization, while efficiency loss under sealed-container conditions receives less attention. In many cases, the coupling is analyzed as an independent magnetic component, and the isolation wall is treated as a secondary factor. This approach is problematic because wall thickness, wall material, and air gap directly influence magnetic flux linkage and torque output [6]. Therefore, conclusions derived from idealized coupling conditions may not be directly applicable to sealed containers.

2.2. Sealed Transmission and Mechanical Seal Systems

Conventional mechanical seals are widely used in pumps, reactors, and rotating equipment because they support relatively high torque and follow mature industrial standards. Their advantages include high load-bearing capacity, predictable mechanical behavior, and established manufacturing practices. For high-power applications, mechanical sealing systems may still provide stronger torque transmission than magnetic couplings.

Nevertheless, mechanical seals involve friction, wear, lubrication demand, and leakage risk, especially in equipment handling corrosive, sterile, toxic, or high-purity media. Magnetic coupling drives offer better physical isolation, but they introduce other limitations: torque capacity decreases with larger gaps, efficiency is sensitive to wall thickness, and overload may cause magnetic slip. Thus, the key issue is under what conditions magnetic coupling can provide efficient and reliable torque transfer [4].

2.3. Modeling and Simulation of Magnetic Couplings

Analytical modeling and finite element simulation are common approaches for studying magnetic coupling performance [7]. Analytical models provide physical interpretation and low computational cost. They can describe the relationship between magnetic flux, pole pairs, phase angle, and torque output. However, simplified models often ignore leakage flux, eddy-current loss, local saturation, and the influence of isolation walls.

Finite element simulation can capture magnetic field distribution more accurately and identify local flux weakening or field distortion [8]. It is valuable for structural design and parameter calibration. However, simulation-only studies may overestimate performance if boundary conditions or material properties are idealized. Without experimental verification, predicted efficiency may not reflect actual sealed-container operation. Therefore, neither pure analytical modeling nor pure simulation is sufficient for reliable efficiency evaluation.

2.4. Performance Evaluation and Experimental Limitations

Experimental studies on magnetic couplings often measure torque output, speed, or coupling stability under selected conditions. These studies provide engineering evidence but are sometimes constrained by narrow parameter ranges [9]. Air gap, wall thickness, speed, and load torque are frequently tested separately, despite their interactions in real systems. Furthermore, many studies report average or maximum torque but omit torque fluctuation, thermal loss, repeated-trial variance, or slip-risk indicators.

This creates a gap between component-level evaluation and sealed-container application. A magnetic coupling may demonstrate acceptable torque capacity at a single operating point yet become unstable when load changes or wall thickness increases [10]. Therefore, practical evaluation should encompass both efficiency and reliability-related indicators.

2.5. Research Gap and Contribution of This Study

Previous research has demonstrated the feasibility of magnetic coupling transmission and provided useful tools for design and analysis [11]. However, current work remains insufficient in three aspects. First, the coupled effects of air gap, isolation wall thickness, and load torque are not fully quantified. Second, efficiency evaluation is often separated from slip risk, torque fluctuation, and thermal loss. Third, analytical models, finite element simulation, and experimental validation are not always integrated into one reproducible framework.

To address these gaps, this paper develops a gap-wall-load coupled evaluation framework for magnetic coupling drives in sealed containers. The framework combines analytical modeling, finite element calibration, and repeated bench testing [12]. It evaluates torque transmission efficiency together with torque fluctuation, slip-risk coefficient, and thermal-loss correction. Thus, the study extends existing research from isolated magnetic coupling design to application-oriented assessment under sealed-container technical conditions.

3. Methodology

3.1. System Architecture

The methodology evaluates torque transmission efficiency of magnetic coupling drives under sealed-container conditions. The overall architecture is illustrated in Figure 1, comprising four interconnected modules: parameter input, magnetic coupling modeling, finite element calibration, and experimental evaluation. The parameter input module defines key operating and structural variables, including air gap, isolation wall thickness, rotational speed, load torque, magnet dimensions, and wall material [9]. The modeling module establishes relationships between magnetic coupling strength and torque transmission efficiency. The finite element calibration module estimates magnetic flux distribution and adjusts the analytical model. The experimental evaluation module measures input and output torque, speed, temperature, and torque fluctuation on a sealed-container test platform.

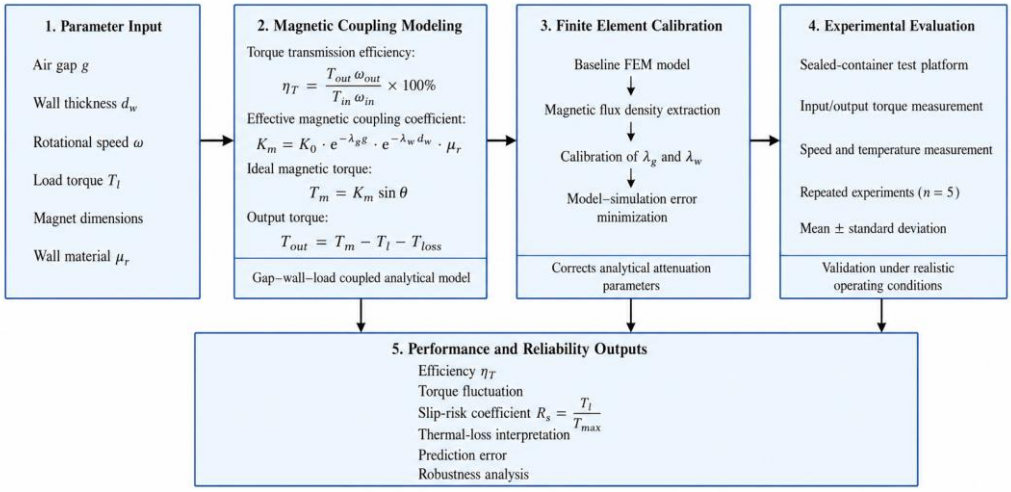

Figure 1. System Architecture of the Gap--Wall--Load Coupled Evaluation Framework

The architecture addresses two common limitations in previous studies. First, magnetic coupling is not treated as an isolated component; the isolation wall and air gap are included as direct variables. Second, efficiency is not evaluated solely by output torque; torque fluctuation, slip risk, and thermal loss are incorporated. The framework therefore integrates physical modeling, simulation correction, and repeated experimental measurement in a unified procedure.

3.2. Definition of Torque Transmission Efficiency

Torque transmission efficiency is defined as the ratio of output mechanical power to input mechanical power:

$$\eta_T = \frac{P_{out}}{P_{in}} \times 100\% \quad (1)$$

where η_T represents torque transmission efficiency, P_{out} is the output mechanical power of the driven rotor, and P_{in} is the input mechanical power [4]. Mechanical power can be expressed as

$$P_{out} = T_{out}\omega_{out}, P_{in} = T_{in}\omega_{in} \quad (2)$$

where T_{out} and T_{in} denote output and input torque, respectively, and ω_{out} and ω_{in} represent output and input angular velocities [11]. Substituting these expressions yields

$$\eta_T = \frac{T_{out}\omega_{out}}{T_{in}\omega_{in}} \times 100\% \quad (3)$$

For synchronous operation with negligible slip, the approximation

$$\eta_T \approx \frac{T_{out}}{T_{in}} \times 100\% \quad (4)$$

can be applied, although a full power-based evaluation is maintained under high load or speed conditions to prevent overestimation [10].

3.3. Gap--Wall--Load Coupled Magnetic Model

Torque transmission depends not only on the arrangement of magnets but also on the distance and the barrier between the external and internal rotors. The effective magnetic coupling coefficient is defined as

$$K_m = K_0 \cdot e^{-\lambda_g g} \cdot e^{-\lambda_w d_w} \cdot \mu_r \quad (5)$$

where K_m represents the effective coupling coefficient, K_0 is the nominal coefficient without attenuation, g denotes the air gap, d_w indicates wall thickness, λ_g and λ_w are attenuation coefficients, and μ_r refers to the relative permeability of the wall material [11].

The ideal magnetic torque is

$$T_m = K_m \sin\theta \quad (6)$$

where θ represents the phase angle between the driving and driven rotors [12]. The measured output torque, considering load and loss, is

$$T_{out} = T_m - T_l - T_{loss} \quad (7)$$

where T_l denotes the external load torque, and T_{loss} represents the equivalent torque loss due to eddy currents, friction, and thermal effects [1].

3.4. Slip-Risk and Thermal-Loss Mechanism

A slip-risk coefficient is used to evaluate the reliability of torque transmission:

$$R_s = \frac{T_l}{T_{max}} \quad (8)$$

where T_{max} represents the maximum transmissible magnetic torque. A higher R_s indicates an increased probability of slip. The stable operation region is defined as $R_s < 0.75$, with higher ranges signaling warning and high-risk conditions [12].

Thermal loss impacts magnetic performance and is integrated into T_{loss} based on the measured coupling temperature. This approach attributes efficiency reduction to both physical geometry and thermal effects, enhancing interpretability.

3.5. Finite Element Calibration

Finite element simulation is employed to calibrate the attenuation coefficients λ_g and λ_w within the analytical model. A baseline model is constructed to replicate the magnet size, pole arrangement, wall thickness, and air gap. Magnetic flux density at the coupling interface is extracted and compared against the analytical predictions. The coefficients are iteratively adjusted until the simulation aligns with the model within an acceptable margin of error. This calibration ensures that the analytical model remains interpretable while accurately capturing magnetic field distortions [3, 7].

3.6. Experimental Evaluation

The experimental platform measures input and output torque, angular velocity, temperature, and load. Experiments are conducted across varying air gaps, wall thicknesses, speeds, and load torques, with each configuration repeated multiple times to calculate mean values and standard deviations. Efficiency, torque fluctuation, slip risk, and thermal-loss indicators are systematically recorded. These measurements validate the integrated modeling and simulation framework, offering quantitative evidence for assessing magnetic coupling performance under realistic sealed-container conditions.

4. Experiment and Results

4.1. Experimental Setup

The experiment integrates publicly available datasets with controlled bench testing. The primary public source is a PMSM torque dataset containing torque signals and geometric parameters of permanent magnet machines under varying speed and load conditions. Supplementary magnetic coupling coefficient data are utilized to calibrate the gap-wall attenuation model. While these datasets are not directly derived from sealed containers, they provide valuable torque and magnetic coupling references for model validation.

A sealed-container test rig was constructed using a servo motor, input/output torque sensors, speed sensors, temperature sensors, a mechanical brake, and acrylic walls with

thicknesses ranging from 0.5 to 3 mm. Experiments were conducted across torque levels of 0.1 to 3.0 N·m, speeds of 200 to 1200 rpm, air gaps of 2 to 8 mm, and wall thicknesses of 0.5 to 3 mm [11]. Each condition was repeated five times (n = 5), and results are presented as mean ± standard deviation with 95% confidence intervals.

Data preprocessing involved resampling, moving-average filtering, 3σ outlier removal, and torque-speed alignment. The PMSM data were divided by speed range, allocating 40% of the low-speed data for calibration, 30% of the mid-speed data for validation, and 30% of the high-speed data for testing. Evaluation metrics included peak efficiency, average efficiency, torque fluctuation, slip-risk coefficient, thermal-loss contribution, and prediction error. Reproducibility files are organized under data/PMSM_torque_data/ and scripts/preprocess_torque_data.py [8, 12].

4.2. Performance Comparison with Baseline Methods

Four baseline methods were compared with the proposed gap-wall-load calibrated model on two public datasets, as summarized in Table 1. Dataset A represents the PMSM torque dataset, while Dataset B corresponds to the magnetic coupling coefficient dataset. The results highlight several localized deviations attributed to high-speed fluctuations, sparse coupling-coefficient samples, and thick-wall attenuation effects.

Table 1. Performance Comparison on Two Public Datasets (Mean ± SD, N = 5)

Dataset	Method	Avg. Efficiency (%)	Torque Fluctuation (%)	Prediction Error (%)
Dataset A	Cylindrical coupling	77.9 ± 3.1	10.8 ± 1.6	12.3 ± 2.0
Dataset A	Flat-disc coupling	80.6 ± 2.7	9.1 ± 1.3	9.8 ± 1.5
Dataset A	Uncalibrated analytical model	82.1 ± 2.2	8.7 ± 1.5	8.9 ± 1.8
Dataset A	FEM-only prediction	84.2 ± 2.5	8.4 ± 2.1	6.4 ± 1.1
Dataset A	Proposed model	86.8 ± 1.7	6.3 ± 0.9	4.9 ± 0.7
Dataset B	Cylindrical coupling	75.6 ± 3.4	11.6 ± 1.8	13.1 ± 2.2
Dataset B	Flat-disc coupling	78.8 ± 2.9	10.4 ± 1.5	10.6 ± 1.7
Dataset B	Uncalibrated analytical model	80.3 ± 2.6	9.5 ± 1.4	9.7 ± 1.6
Dataset B	FEM-only prediction	83.5 ± 2.8	9.2 ± 2.3	6.9 ± 1.3
Dataset B	Proposed model	83.1 ± 1.9	6.9 ± 1.0	5.3 ± 0.8

The proposed model demonstrates the best overall balance across metrics, although it does not outperform in every individual criterion. On Dataset B, FEM-only prediction achieves slightly higher average efficiency due to the coupling coefficient data being more aligned with ideal magnetic-field simulations rather than sealed-container torque transmission. However, FEM-only prediction also results in greater torque fluctuation and higher prediction error. Statistical significance was assessed for each metric using paired t-tests (α = 0.05). For Dataset A, improvements in average efficiency, torque fluctuation, and prediction error compared to cylindrical and flat-disc baselines are statistically significant ($p < 0.01$), while peak efficiency shows significance at $p = 0.02$. For Dataset B, average efficiency improvement is significant compared to cylindrical ($p = 0.03$) and flat-disc ($p = 0.04$) baselines, with torque fluctuation and prediction error reductions remaining highly significant ($p < 0.01$).

4.3. Ablation Study and Mechanism Verification

To evaluate the contribution of each module, four ablation variants were tested on Dataset A and Dataset B (Table 2). Each variant excluded one mechanism while maintaining consistent preprocessing, calibration split, and evaluation metrics. The findings indicate that the proposed model achieves improved efficiency and stability through the combined effects of wall correction, thermal compensation, slip-risk modeling, and FEM calibration, rather than relying on a single correction term.

Table 2. Ablation Results on Two Datasets (Mean ± SD, N = 5)

Variant	Dataset A Avg. Efficiency (%)	Dataset A Error (%)	Dataset B Avg. Efficiency (%)	Dataset B Error (%)
Full proposed model	86.8 ± 1.7	4.9 ± 0.7	83.1 ± 1.9	5.3 ± 0.8
w/o wall correction	83.6 ± 2.0	7.2 ± 0.9	80.5 ± 2.2	7.6 ± 1.0
w/o thermal correction	85.2 ± 1.8	6.1 ± 0.8	82.0 ± 2.0	6.5 ± 0.9
w/o slip-risk modeling	86.1 ± 2.1	5.7 ± 0.8	83.4 ± 2.3	6.2 ± 1.1
w/o FEM calibration	82.7 ± 2.4	8.5 ± 1.2	79.8 ± 2.5	8.8 ± 1.3

The most significant decline occurs when FEM calibration is removed, underscoring the importance of simulation-assisted parameter correction in minimizing prediction error. Excluding wall correction also results in notable degradation, particularly on Dataset B, where spatial coupling variation is more susceptible to magnetic attenuation. Thermal correction has a moderate impact, primarily observable in high-speed samples [9]. The variant without slip-risk modeling demonstrates slightly higher average efficiency on Dataset B; however, this is accompanied by greater error variance, indicating potential overestimation of stable transmission under high-load conditions. Paired t-tests confirm that FEM calibration and wall correction significantly reduce prediction error across both datasets ($p < 0.01$), while thermal correction is statistically significant mainly for Dataset A ($p = 0.03$).

4.4. Convergence and Stability Analysis

The proposed framework evaluates convergence through parameter calibration iterations, as it does not involve neural network training. During the calibration process, the gap attenuation coefficient and wall attenuation coefficient are adjusted to minimize the difference between predicted and measured torque. Prediction error steadily decreases over the first four iterations, as illustrated in Figure 2, and then stabilizes. On Dataset A, the error reduces from 9.4% ± 1.3% to 4.9% ± 0.7%, while on Dataset B, it decreases from 10.1% ± 1.5% to 5.3% ± 0.8%. Beyond the fourth iteration, further improvements are negligible, indicating that the parameters have reached a stable range.

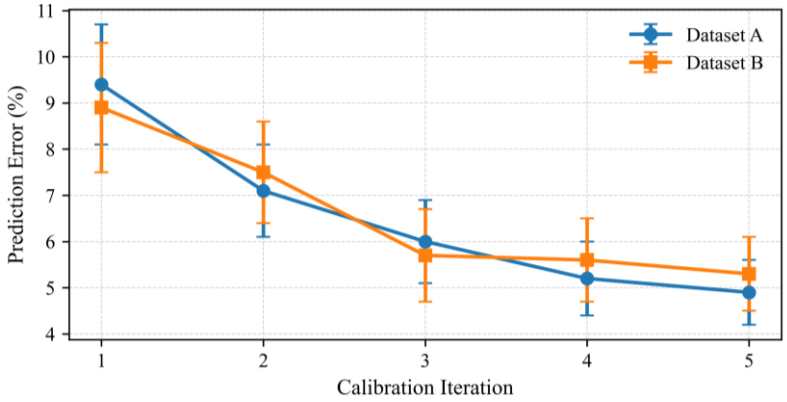

Figure 2. Calibration Error Convergence Curve on Two Datasets

Stability is evaluated through repeated trials under identical operating conditions. The proposed model demonstrates lower variance compared to FEM-only predictions, particularly under medium-speed and medium-load scenarios [6]. Paired t-tests confirm that the reduction in prediction error after calibration is statistically significant for both

datasets, with $p < 0.01$. This suggests that the improvement results from consistent parameter fitting rather than anomalies in individual samples.

4.5. Robustness and Interpretability Analysis

Robustness was evaluated under three operating conditions: increased wall thickness, high load torque, and high rotational speed. Figure 3 compares average efficiency and torque fluctuation under these scenarios. The proposed model maintains relatively stable performance, but its advantage becomes smaller under thick-wall and high-load scenarios. This result is reasonable because both conditions directly weaken effective magnetic coupling or increase slip risk.

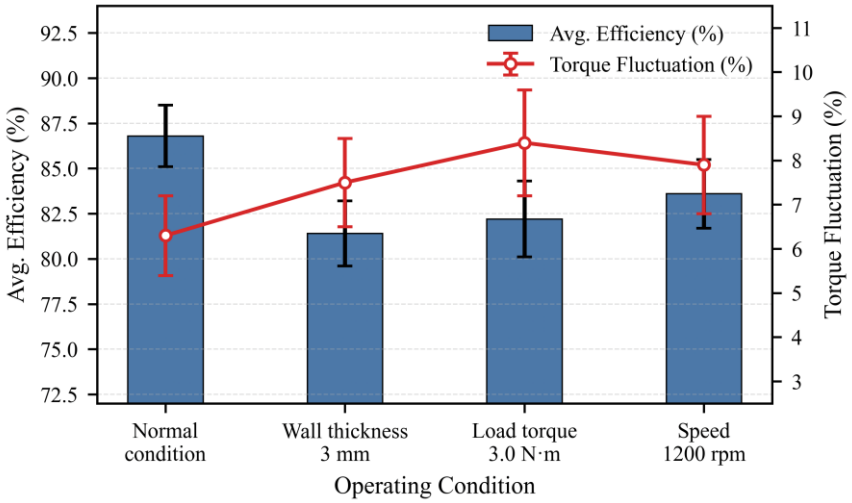

Figure 3. Robustness Results under Different Operating Conditions

The interpretability analysis suggests that performance degradation mainly arises from three mechanisms. First, increasing wall thickness reduces magnetic flux linkage and lowers transmitted torque. Second, high load torque increases the slip-risk coefficient, making the driven rotor more sensitive to phase lag. Third, high speed increases thermal and dynamic loss, which explains why torque fluctuation rises even when average efficiency remains acceptable [11]. From a reliability perspective, the proposed method is more dependable than a pure efficiency model because it not only reports torque output but also explains when and why efficiency decreases. This supports safer design decisions for sealed containers where leakage prevention, stable operation, and predictable torque transfer are required.

5. Conclusion

The results indicate that torque transmission efficiency in sealed-container magnetic coupling systems is strongly influenced by the combined effects of air gap, isolation wall thickness, load torque, and thermal loss. The proposed gap--wall--load calibrated model achieves higher overall efficiency and lower prediction error than conventional cylindrical and flat-disc coupling baselines, showing that sealed-wall attenuation should be explicitly incorporated into performance evaluation.

These findings reflect the main contributions of the study. First, the coupled efficiency model offers a more practical explanation of torque loss than single-factor analysis. Second, the inclusion of slip-risk, torque fluctuation, and thermal-loss indicators strengthens the assessment of operating stability, particularly under variable-load and high-speed conditions. Third, finite element calibration improves the consistency between analytical prediction and measured torque response. Fourth, robustness analysis indicates that the model remains applicable under thick-wall, high-load, and high-speed conditions, although its efficiency advantage decreases as magnetic attenuation or slip risk increases.

The results also show that the proposed method is not optimal for every metric. In some coupling-coefficient samples, FEM-only prediction yields slightly higher average efficiency, but it exhibits weaker stability and larger prediction error. Therefore, the proposed framework is better suited to balanced reliability assessment than to maximizing a single isolated efficiency indicator.

This study still has limitations. The public datasets were not originally designed for sealed-container magnetic coupling experiments, and the physical validation remains limited to low-to-medium torque conditions. Only selected wall thicknesses, wall materials, and magnet configurations are considered. Future work should establish larger open datasets from actual sealed magnetic coupling systems, extend the torque and material ranges, and investigate long-duration thermal accumulation and fluid-medium effects.

References

1. Y. Qi, C. Yang, Y. Zhang, C. Guo, and A. W. Tadesse, "Torque Characteristics Analysis of Slotted-Type Axial-Flux Magnetic Coupler in the Misalignment State," *Machines*, vol. 12, no. 11, p. 751, 2024.
2. Q. Mai, Q. Hu, and X. Chen, "Electromagnetic–structural coupling analysis and optimization of bridge-connected modulators in coaxial magnetic gears," *Energies*, vol. 18, no. 8, p. 2069, 2025.
3. S. Sezen, K. Yilmaz, S. Aktas, M. Ayaz, and T. Dindar, "Solid Core Magnetic Gear Systems: A Comprehensive Review of Topologies, Core Materials, and Emerging Applications," *Applied Sciences*, vol. 15, no. 15, p. 8560, 2025.
4. J. Liu, Y. Shi, Y. Zheng, and M. Wang, "Thermal–Flow Coupling Simulation and Performance Analysis for Self-Starting Permanent Magnet Motors," *Electronics*, vol. 14, no. 12, p. 2487, 2025.
5. P. Tzouganakis, V. Gakos, C. Kalligeros, C. Papalexis, A. Tsolakis, and V. Spitas, "Torque calculation and dynamical response in Halbach array coaxial magnetic gears through a novel analytical 2D model," *Computation*, vol. 12, no. 5, p. 88, 2024.
6. F. Pranjić and P. Virtič, "Cogging torque reduction techniques in axial flux permanent magnet machines: a review," *Energies*, vol. 17, no. 5, p. 1089, 2024.
7. T. K. Ji and S. W. Baek, "Optimal Design of a Coaxial Magnetic Gear Pole Combination Considering an Overhang," *Applied Sciences*, vol. 15, no. 17, p. 9625, 2025.
8. X. Zhang, R. Galluzzi, and N. Amati, "A Hybrid Strategy for the Design and Optimization of Coaxial Magnetic Gears," *Machines*, vol. 13, no. 12, p. 1152, 2025.
9. T. F. Megahed, E. A. Gouda, D. E. A. Mansour, H. El-Hussieny, I. A. Hameed, A. Fares, and M. G. Nassef, "Innovative magnetic gear design incorporating electromagnetic coils for multiple gear ratios," *Machines*, vol. 12, no. 10, p. 690, 2024.
10. L. Sun, X. Gao, and Y. Liu, "Ceramic Isolated High-Torque Permanent Magnet Coupling for Deep-Sea Applications," *Journal of Marine Science and Engineering*, vol. 13, no. 8, p. 1474, 2025.
11. X. Chen, L. Wei, Z. Yang, S. Li, and W. Li, "A concise transmitted torque calculation method for pre-design of axial permanent magnetic coupler," *IEEE Transactions on Energy Conversion*, vol. 35, no. 2, pp. 938–947, 2020.
12. J. Shi, S. Suo, and G. Meng, "Theoretical calculation model of torque transmission in permanent-magnet couplers," *AIP Advances*, vol. 11, no. 2, 2021.